Geophysical Research Letters

RESEARCH LETTER
10.1029/2022GL100223

**Key Points:**

- Surface and tropospheric ozone has risen significantly over Southeast Asia from 2005 to 2016
- $NO_x$ emission trends underestimated over Peninsular Southeast Asia but overestimated over Maritime Continents in inventories
- Growing anthropogenic emissions drove large surface ozone increases over Peninsular Southeast Asia

**Supporting Information:**

Supporting Information may be found in the online version of this article.

**Correspondence to:**

T.-M. Fu and L. Zhang,
fuzm@sustech.edu.cn;
zhanglg@pku.edu.cn

**Citation:**

Wang, X., Fu, T.-M., Zhang, L., Lu, X., Liu, X., Amnuaylojaroen, T., et al. (2022). Rapidly changing emissions drove substantial surface and tropospheric ozone increases over Southeast Asia. *Geophysical Research Letters*, *49*, e2022GL100223. https://doi.org/10.1029/2022GL100223

Received 7 JUL 2022
Accepted 24 SEP 2022



# Rapidly Changing Emissions Drove Substantial Surface and Tropospheric Ozone Increases Over Southeast Asia

**Xiaolin Wang[1], Tzung-May Fu[2,3], Lin Zhang[1], Xiao Lu[4], Xiong Liu[5], Teerachai Amnuaylojaroen[6], Mohd Talib Latif[7], Yaping Ma[8], Lijuan Zhang[9], Xu Feng[10], Lei Zhu[2,3], Huizhong Shen[2,3], and Xin Yang[2,3]**

[1]Department of Atmospheric and Oceanic Sciences, School of Physics, Peking University, Beijing, China, [2]School of Environmental Science and Engineering, Southern University of Science and Technology, Shenzhen, China, [3]Guangdong Provincial Observation and Research Station for Coastal Atmosphere and Climate of the Greater Bay Area, Southern University of Science and Technology, Shenzhen, China, [4]School of Atmospheric Sciences, Sun Yat-sen University, Zhuhai, China, [5]Harvard & Smithsonian Center for Astrophysics, Cambridge, MA, USA, [6]Department of Environmental Science, School of Energy and Environment, University of Phayao, Phayao, Thailand, [7]Department of Earth Sciences and Environment, Faculty of Science and Technology, Universiti Kebangsaan Malaysia, Bangi, Malaysia, [8]National Meteorological Information Center, China Meteorological Administration, Beijing, China, [9]Shanghai Central Meteorological Observatory, Shanghai, China, [10]John A. Paulson School of Engineering and Applied Sciences, Harvard University, Cambridge, MA, USA

**Abstract** We combined observations and simulations to assess tropospheric ozone trends over Southeast Asia from 2005 to 2016. Multi-platform observations showed that surface ozone had been increasing at rates of 0.7–1.2 ppb $year^{-1}$ over the Peninsular Southeast Asia (PSEA) and 0.2–0.4 ppb $year^{-1}$ over the Maritime Continents (MC); tropospheric ozone columns had been rising throughout Southeast Asia by 0.21–0.35 DU $year^{-1}$. These observed ozone trends were better reproduced by simulations driven with satellite-constrained $NO_x$ emissions, indicating that $NO_x$ emission growths may have been underestimated for the PSEA and overestimated for the MC in the Community Emissions Data System and the Global Fire Emissions Data set. The surface ozone increases over the PSEA were driven by rapidly growing local emissions, wherein fire emission growths may still be underestimated even with satellite constraints. We highlighted the need for better quantifying Southeast Asian emissions to benefit air quality management.

**Plain Language Summary** Tropospheric ozone at individual locations in Southeast Asia has reportedly been rising in recent decades, but the spatiotemporal characteristics and causes of such increases have not been assessed. We combined model simulations with surface, airborne, and satellite observations to assess the trends of surface and tropospheric ozone over Southeast Asia from 2005 to 2016. Surface and tropospheric ozone concentrations have risen throughout Southeast Asia, albeit with spatially and seasonally inhomogeneous trends. We showed that current emission inventories based on activity statistics may have underestimated the emission growths in the Peninsular Southeast Asia while overestimated the emission growths in the Maritime Continents. Emission inventories should be re-evaluated to help guide air quality management in this region.

## 1. Introduction

Tropospheric ozone is an air pollutant, a greenhouse gas, and an oxidant affecting climate and chemistry (Monks et al., 2015). Tropospheric ozone is mainly produced by the oxidation of CO and volatile organic compounds (VOCs) in the presence of nitrogen oxides ($NO_x = NO + NO_2$) and sunlight, with minor contributions from stratospheric transport (Monks et al., 2015). Regional tropospheric ozone abundances are thus affected by variations in precursor emissions, photochemistry, and atmospheric dynamics. In Southeast Asia (Figure S1 in Supporting Information S1), including the Peninsular Southeast Asia (PSEA) and the Maritime Continent (MC, here referring to Malaysia, Singapore, Indonesia, and Brunei), tropospheric and surface ozone concentrations have reportedly been increasing at individual locations in recent decades (Gaudel et al., 2018, 2020; IPCC, 2021). However, the long-term ozone trends across Southeast Asia and the drivers of such trends have not been systematically assessed, impeding effective air quality management in the region.

Long-term measurements of surface and tropospheric ozone over Southeast Asia have been relatively scarce, and published analyses have not shown consistent ozone trends. Measurements in Eastern Thailand showed that surface ozone during the dry season (November to the following March) had risen significantly between 1997 and 2012 (Assareh et al., 2016). In contrast, surface ozone concentrations over the Malaysian Peninsula and the Malaysian Borneo had shown small or insignificant trends between 1997 and 2016 (Ahamad et al., 2020; Latif et al., 2016). Analyses of tropospheric column ozone (TCO) in six satellite retrievals (from two satellite instruments) and one trajectory-mapped ozonesonde data set showed positive TCO trends (0.1–0.8 DU year$^{-1}$) between 2003 and 2016 over southern PSEA, but the datasets differed on the signs of TCO trends over the MC (Gaudel et al., 2018; Ziemke et al., 2019). Gaudel et al. (2020) analyzed ozone measurements onboard commercial aircrafts and reported ozone increases throughout the troposphere at rates of 5.8 $\pm$ 1.7 ppb decade$^{-1}$ over Malaysia and Indonesia and 5.4 $\pm$ 1.2 ppb decade$^{-1}$ over the PSEA during 1994–2016. However, their analysis over the PSEA included measurements over Southern China and may be affected by the known Chinese tropospheric ozone increases (Lu et al., 2020; Wang et al., 2019).

Interannual variations in emissions and meteorology may drive ozone trends over Southeast Asia, but their individual contributions have not been assessed. Satellite-observed tropospheric $NO_2$ column concentrations had increased substantially over the PSEA and mildly over the MC from 1996 to 2017 (Georgoulias et al., 2019) due to growing regional population and energy demands (International Energy Agency, 2019; Kurokawa & Ohara, 2020). Such rising precursor emissions might have led to disproportional tropospheric ozone increases, as ozone photochemical production is faster and more $NO_x$-sensitive in the tropics (Y. Zhang et al., 2016, 2021). Biomass burning over Southeast Asia, which is strongly modulated by ENSO (Y. Chen et al., 2017; van der Werf et al., 2008), has been shown to adversely affect local air quality (Amnuaylojaroen et al., 2019; Khodmanee & Amnuaylojaroen, 2021; Reddington et al., 2021), and the transformation of natural forests to croplands and oil palm plantations might have magnified these adverse impacts (Austin et al., 2019; Oanh et al., 2018). The background ozone levels in Southeast Asia are also affected by the interannual variations of the Asian monsoon and tropical climate, which modulate the photochemistry and transport of ozone and its precursors (Ashfold et al., 2017; Olsen et al., 2016; Oman et al., 2013; Sekiya & Sudo, 2012).

In this study, we conducted an integrated analysis of ozone observations from surface sites, aircraft, ozonesondes, and satellite instruments over Southeast Asia from 2005 to 2016 to quantify the regional ozone trends. We conducted sensitivity simulations using bottom-up and top-down precursor emissions to attribute the observed ozone trends to interannual variations of emissions and meteorology.

## 2. Data and Methods

### 2.1. Surface and Tropospheric Ozone Measurements

We compiled a database of all obtainable in situ ozone measurements over Southeast Asia from 2005 to 2016. Seasonal mean daily maximum 8-hr average (MDA8) surface ozone concentrations at 34 sites (7 in the PSEA and 27 in the MC, Figure S1 in Supporting Information S1) were calculated from hourly measurements using a consistent quality control protocol (Text S1 and Table S1 in Supporting Information S1). Ozonesonde and aircraft observations of ozone vertical profiles over Southeast Asia were from the Southern Hemisphere Additional Ozonesondes (SHADOZ) (Thompson et al., 2017; Witte et al., 2017, 2018) and the In-service Aircraft for the Global Observing System (IAGOS) (Nédélec et al., 2015; Petzold et al., 2015) datasets. In all, we included 727 ozone profiles over the PSEA (498 profiles over Bangkok, Thailand; 229 profiles over Hanoi, Vietnam) and 321 ozone profiles over the MC (all over Kuala Lumpur, Malaysia), with 19–100 profiles at each site in each season (Text S2 and Table S2 in Supporting Information S1).

We analyzed satellite observations of TCO over Southeast Asia from 2005 to 2016 using the Ozone Monitoring Instrument (OMI) Level 2 Ozone Profile product (OMPROFOZ) retrieved by the Smithsonian Astrophysical Observatory algorithm (hereafter referred to as OMI/SAO), gridded to 2.5° longitude × 2° latitude resolution and 24 vertical layers (X. Liu et al., 2010). The TCO trends calculated from the raw OMI/SAO product contained systematic positive biases due to instrument degradation and row anomalies (Huang et al., 2017). We removed these systematic biases by aligning the global zonal-mean TCO seasonal trends calculated from the OMI/SAO product to those calculated from the OMI/MLS product (Ziemke et al., 2019) (Text S3 in Supporting Information S1).

Tropospheric $NO_2$ column concentrations from 2005 to 2016 were from the NASA OMI $NO_2$ Standard Product (OMNO2) (Krotkov et al., 2017) with daily global coverage and 13 × 24 km spatial resolution at nadir. We re-gridded the monthly mean tropospheric $NO_2$ column concentrations to 0.5° × 0.625° resolution for comparison with our model simulations (Text S4 in Supporting Information S1).

### 2.2. GEOS-Chem Simulations of Tropospheric Ozone Using Bottom-Up and Top-Down Precursor Emissions Over Southeast Asia

We simulated tropospheric ozone over Southeast Asia between 2005 and 2016 using the GEOS-Chem global 3-D chemical transport model version 12.1.1 (Bey et al., 2001; www.geos-chem.org) with 2.5°longitude × 2°latitude horizontal resolution and 47 vertical layers. GEOS-Chem included detailed tropospheric $HO_x$-$NO_x$-VOC-ozone-halogen-aerosol chemistry (Mao et al., 2013; Sherwen et al., 2016). Stratospheric chemistry was simulated using the linearized ozone parameterization (McLinden et al., 2000). The simulations were driven by assimilated meteorology from the NASA Modern-Era Retrospective Analysis for Research and Applications, Version 2 (MERRA-2) (Gelaro et al., 2017).

As a starting point for our analyses, we drove the GEOS-Chem model using bottom-up, year-specific monthly emissions of ozone precursors from 2005 to 2016 (Text S5 in Supporting Information S1). Global anthropogenic emissions were from the Community Emissions Data System (CEDS, O'Rourke et al., 2021), with 0.5° native resolution and included emissions from energy production, industry, land transportation, residential and commercial activities, solvent use, agriculture, waste processing, ships, and aircrafts (McDuffie et al., 2020). Ship emissions were injected into model surface grids as chemically aged plumes (Holmes et al., 2014). Biomass burning emissions were from the Global Fire Emissions Data set version 4 with small fires (GFED4s, van der Werf et al., 2017) at 0.25° native resolution and were injected to the model boundary layer following the standard practice in GEOS-Chem. A previous study over Southeast Asia showed that injecting 40% of the biomass burning emissions directly into the free troposphere in the model would result in <5% changes in the simulated surface and tropospheric ozone, compared to a simulation where all biomass burning emissions were released in the boundary layer (Jian & Fu, 2014). Emissions of biogenic VOCs, soil $NO_x$, and lightning $NO_x$ were calculated online (Guenther et al., 2012; Hudman et al., 2012; Murray et al., 2012). For comparison against the OMI-observed TCO, we convoluted the simulated monthly ozone profiles (at OMI overpass time) with the monthly mean averaging kernels (AKs) and *a priori* ozone profiles of the OMI/SAO retrievals (L. Zhang et al., 2010).

We hypothesized that the interannual variations of anthropogenic and biomass burning $NO_x$ emissions might be key drivers for the ozone trends over Southeast Asia. However, previous studies and our preliminary analysis of the simulated tropospheric $NO_2$ trends (Text S4 in Supporting Information S1) indicated that the $NO_x$ emission growths over Southeast Asia were not correctly represented in the bottom-up inventories (Elguindi et al., 2020; Goldberg et al., 2021). We thus designed a "top-down" simulation, where we scaled the anthropogenic and biomass burning emissions of $NO_x$ over Southeast Asia with OMI-observed $NO_2$ trends (Texts S4 and S6 in Supporting Information S1). The top-down $NO_x$ emission trend over the PSEA (93.6 Gg NO $year^{-1}$) was 48% larger than the bottom-up trend (63.3 Gg NO $year^{-1}$), but the top-down $NO_x$ emission trend over the MC (20.1 Gg NO $year^{-1}$) was 87% lower than the bottom-up trend (158.1 Gg NO $year^{-1}$) (Figure S2 in Supporting Information S1).

On the basis of our simulation driven with top-down emissions, we further conducted four sensitivity experiments (Table S3 in Supporting Information S1), each removing the interannual variation of emissions from one of the following sources (by fixing the emissions from that source at year-2005 levels): (a) anthropogenic emissions in Southeast Asia (except aircraft emissions), (b) anthropogenic emissions from the rest of the world (except aircraft emissions), (c) global aircraft emissions, and (d) global biomass burning emissions. The individual contributions of these factors to the Southeast Asian ozone trends could be estimated by the differences between these sensitivity experiments and the top-down simulation. We attributed the remaining ozone trends not contributed by any of the above drivers to the interannual variation of meteorology.

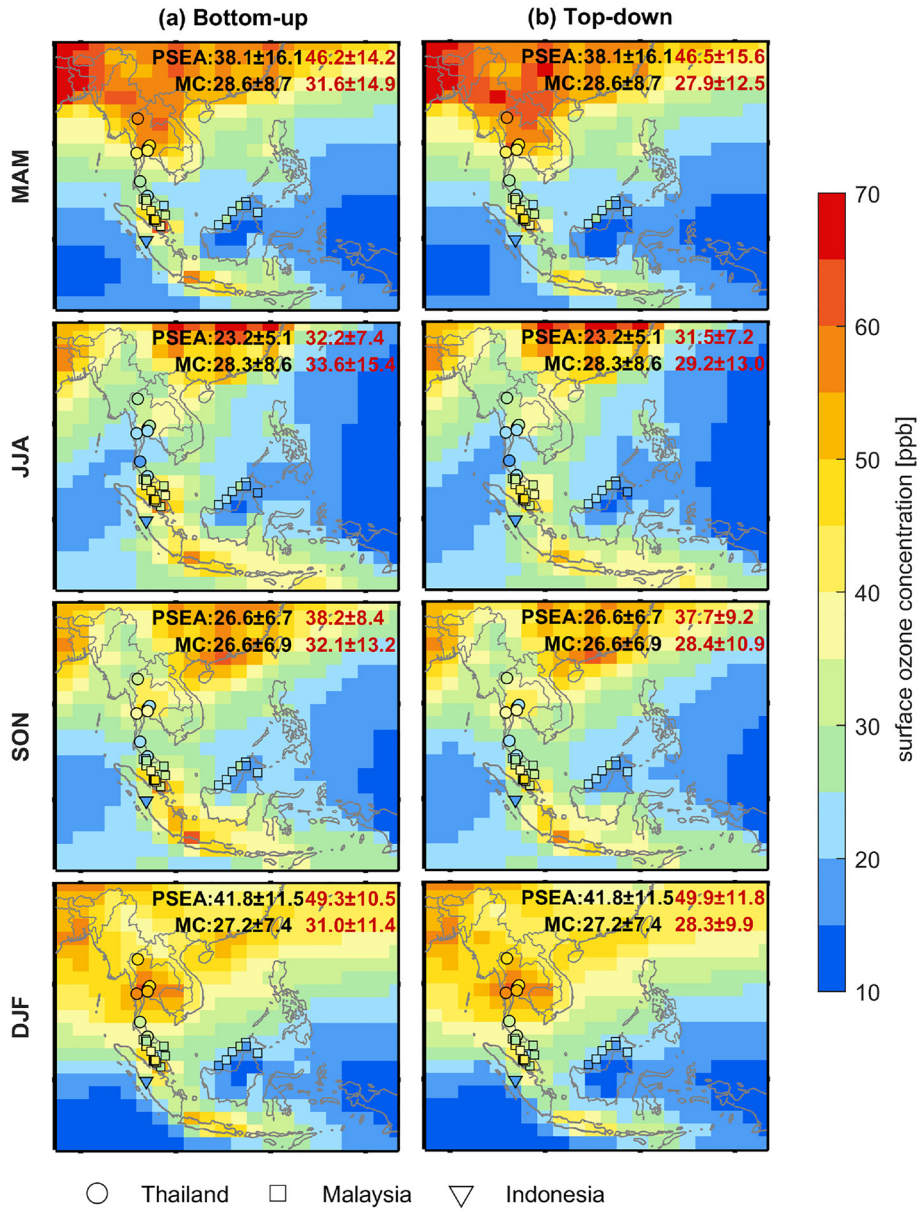


**Figure 1.** Comparison of observed (symbols, country-coded) and simulated (filled pixels) seasonal mean maximum daily 8-hr average (MDA8) surface ozone concentrations over Southeast Asia for the years 2005–2016: (a) simulation driven by bottom-up emissions, (b) simulation driven by top-down emissions. Mean values and standard deviations of observed (black) and simulated (red) seasonal MDA8 ozone concentrations are shown inset.

## 3. Evaluation of Simulated Seasonal Surface and Tropospheric Ozone Over Southeast Asia

### 3.1. Observed and Simulated Seasonal Surface Ozone Over Southeast Asia

We first examined the spatiotemporal distributions of observed seasonal ozone over Southeast Asia and the GEOS-Chem's ability to reproduce those observed features. Figure 1 and Figure S3 in Supporting Information S1 shows the observed seasonal surface MDA8 ozone concentrations over Southeast Asia averaged from 2005 to 2016. Surface ozone over the PSEA showed substantial seasonal variation, with higher concentrations during the local dry season (38.1 ± 16.1 ppb in MAM and 41.8 ± 11.5 ppb in DJF), reflecting the combined impacts of enhanced biomass burning emissions and stronger photochemistry. During the local wet season (June to November), precipitation and inflow of marine air masses led to lower ozone concentrations over the PSEA (23.2 ± 5.1

ppb in JJA and 26.6 ± 6.7 in SON). Over the MC, the seasonal variation of surface ozone was less prominent, with the observed MDA8 ozone ranging 27.6 ± 7.6 ppb year-round. Surface ozone levels were higher over the Malaysian Peninsula and Java and lower over Sumatra and Borneo, consistent with the distribution of anthropogenic $NO_x$ emissions.

The GEOS-Chem simulations driven by bottom-up or top-down emissions both reproduced the observed spatial and seasonal variations of surface ozone (Figure 1, Figures S3 and S4 in Supporting Information S1). However, the model driven with bottom-up emissions significantly overestimated the observed MDA8 ozone concentrations over the PSEA and the MC in all seasons, with annual mean biases of +9.0 ± 2.0 ppb over the PSEA and +4.5 ± 1.5 ppb over the MC (Figure S3 in Supporting Information S1). Driving the model with top-down emissions reduced the bias over the MC but did not reduce the bias over the PSEA (Figure S3 in Supporting Information S1).

### 3.2. Observed and Simulated Seasonal TCO Over Southeast Asia

Figures S5 and S6 in Supporting Information S1 show the spatial and seasonal variation of TCO as observed by OMI and as simulated by GEOS-Chem over Southeast Asia from 2005 to 2016. The OMI-observed TCO was lower near the Equator and higher toward the northern sub-tropics in all seasons, reflecting the combined effects of the ozone depletion by water vapor in the tropics and the pronounced anthropogenic emissions over East Asia. The observed TCO over the PSEA peaked in MAM (36.6 ± 2.5 DU), reflecting the stronger fire emissions and photochemistry during the local dry season (Marvin et al., 2021). Over the MC, the observed TCO was <30 DU year-round with relatively small seasonal variation. The simulations driven by bottom-up and top-down emissions both captured the latitudinal gradient of TCO and the seasonal variation (Figure S6 in Supporting Information S1). Both simulations showed a slight underestimation of TCO over the tropics with a seasonal bias between −0.9 and −3.9 DU, especially over the MC.

## 4. Observed and Simulated Trends of Tropospheric and Surface Ozone Over Southeast Asia Between 2005 and 2016

### 4.1. Simulated Seasonal Surface Ozone Trends Using Bottom-Up and Top-Down Emission Estimates

Figure 2 compares the observed and simulated trends of seasonal surface MDA8 ozone over Southeast Asia from 2005 to 2016. Over the PSEA, observed seasonal surface ozone concentrations had risen significantly (0.7 ± 0.5 to 1.2 ± 0.6 ppb $year^{-1}$), with more pronounced trends in MAM and DJF. Due to the inhomogeneous distribution of the sites, these observed trends mainly reflected the rapid surface ozone increases over Central and Western Thailand. The one site in Northern Thailand showed only a small positive trend in DJF and no significant trends for the rest of the year. Over the MC, the observed seasonal surface ozone trends ranged from 0.2 ± 0.3 to 0.4 ± 0.3 ppb $year^{-1}$, without substantial seasonal variations but showed considerable spatial variations. Seven out of the 18 sites over Peninsular Malaysia showed increasing surface ozone for all seasons (trends between 0.68 and 0.88 ppb $year^{-1}$, Table S1 in Supporting Information S1). Six sites showed increasing seasonal ozone, and the other five sites showed decreasing or non-significant ozone trends. Eight surface sites in the Malaysian Borneo showed small or insignificant ozone trends. In Indonesia, the only surface site at Bukit Koto Tabang (a suburban location) did not show significant ozone trends in any seasons. Overall, observed surface ozone concentrations during the years 2005–2016 showed consistent increases over Central and Western Thailand, especially during the dry season, and scattered increases over the Peninsular Malaysian and Borneo Malaysia.

The simulation driven by bottom-up emissions showed mild seasonal surface ozone increases over the PSEA (0.4 ± 0.2 to 0.5 ± 0.4 ppb $year^{-1}$), but the simulated trends were smaller than the observed trends in Thailand. Over the MC, the simulations using the bottom-up emissions showed substantial surface ozone increases over Indonesia in all seasons, which were inconsistent with the observations at Bukit Koto Tabang. Over the Malaysian Borneo, the simulated surface ozone trends were generally larger than those observed. Overall, the simulation driven by bottom-up emissions underestimated the observed seasonal ozone trends over the PSEA but overestimated the observed seasonal ozone trends over the MC. These biases in simulated ozone trends persisted in a higher-resolution (0.5° × 0.625°) simulation driven by bottom-up emissions (Figure S7 in Supporting Information S1).

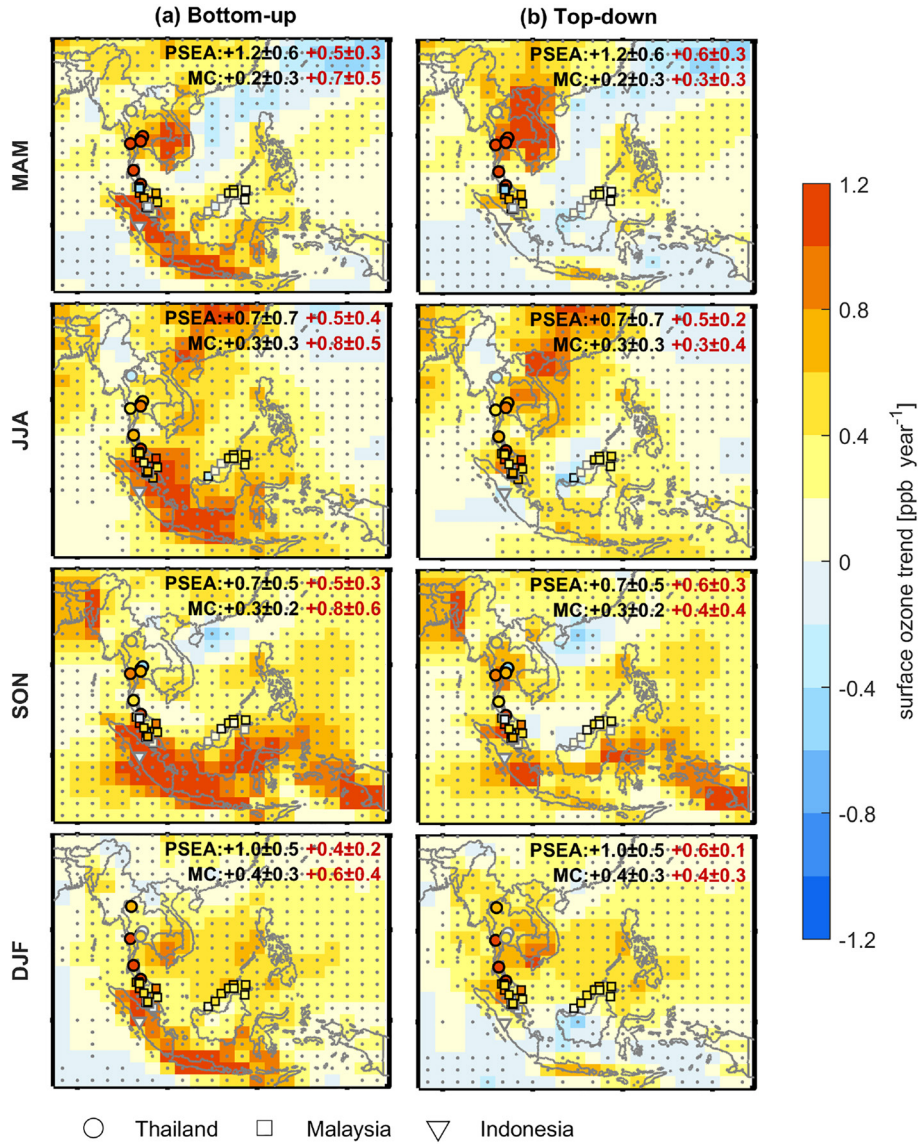


**Figure 2.** Comparison of observed (symbols) and simulated (filled pixels) trends of seasonal mean MDA8 surface ozone concentrations over Southeast Asia for the years 2005–2016: (a) simulation driven by bottom-up emissions, (b) simulation driven by top-down emissions. Symbols with black outlines indicate statistically significant ozone trends (two-tail *t*-test, 0.05 significant level). Dotted pixels indicate significant ozone trends in the simulation. The mean observed (black) and simulated (red, sampled at measurement times and locations) seasonal MDA8 ozone trends are shown inset.

We found that driving the GEOS-Chem model with the top-down emissions led to slightly larger simulated seasonal surface ozone trends across the PSEA (0.5 ± 0.2 to 0.6 ± 0.3 ppb year$^{-1}$, Figure 2b) and much lower simulated seasonal trends over the MC (0.3 ± 0.3 to 0.4 ± 0.4 ppb year$^{-1}$), improving the agreement with observations in both regions. In particular, the surface ozone trends simulated with top-down emissions at Thailand sites (0.20–1.0 ppb year$^{-1}$, Table S1 in Supporting Information S1) were more consistent with the rapid ozone increases observed at those locations.

### 4.2. Evaluation of Observed and Simulated Trends of Tropospheric Ozone

OMI observations showed significant TCO increases throughout Southeast Asia in all seasons between 2005 and 2016 (Figure 3a), with most prominent trends over the PSEA in MAM (0.35 ± 0.16 DU year$^{-1}$) and over the MC in SON (0.37 ± 0.10 DU year$^{-1}$). Figure 3b shows the simulated seasonal TCO trends driven by bottom-up

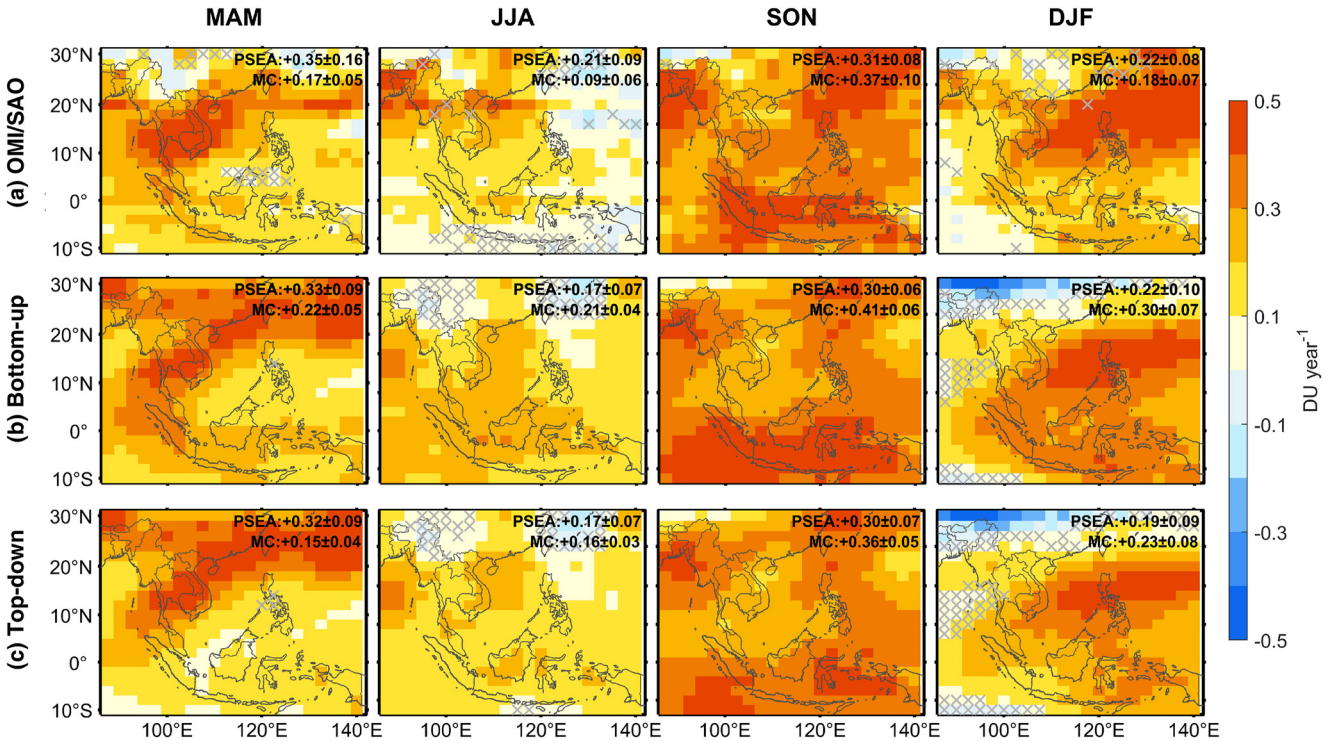


**Figure 3.** Trends of seasonal TCO from 2005 to 2016 (a) as observed by OMI, (b) as simulated with bottom-up emissions, and (c) as simulated with top-down emissions. Hatched grids indicate non-significant TCO trends (two-tail *t*-test, 0.05 significance level). Seasonal TCO trends and their standard deviations are shown inset.

emissions. Over the PSEA, the model shows positive ozone trends of 0.33 ± 0.09 DU year$^{-1}$ in MAM and 0.17 ± 0.07 to 0.30 ± 0.06 DU year$^{-1}$ in other seasons, generally consistent with OMI observations. However, the bottom-up-simulated TCO trends over the MC (0.21 ± 0.04 to 0.41 ± 0.06 DU year$^{-1}$) were considerably exaggerated in all seasons. This positive bias in the simulated MC TCO trends was consistent with that in the simulated surface ozone trends, also implying an overestimation of precursor emission growths in the bottom-up inventories. Using top-down emissions (Figure 3c), the simulated TCO trends over MC were 0.15 ± 0.04 to 0.36 ± 0.05 DU year$^{-1}$, more consistent with the OMI-observed trends in all seasons (0.09–0.37 DU year$^{-1}$).

Ozone vertical profile measurements provided more information on tropospheric ozone change. Figure S8 in Supporting Information S1 shows the observed tropospheric ozone differences over three Southeast Asian sites (Hanoi and Bangkok in the PSEA, and Kuala Lumpur in the MC, Text S2 in Supporting Information S1) between two 5-year periods: March 2005 to February 2010 versus March 2011 to February 2016. Over Bangkok, tropospheric ozone increased substantially throughout the troposphere in most seasons (except JJA) in the latter period relative to the earlier period, although there was considerable observational uncertainty during the earlier period. In particular, lower-tropospheric ozone concentrations during the local dry season (MAM and DJF) increased by >20 ppb, consistent with surface and satellite observations. The observed tropospheric ozone profiles over Hanoi did not show significant differences between the two periods, inconsistent with the TCO increases in the OMI observations. Over Kuala Lumpur, observed ozone profiles showed >10 ppb ozone increases throughout the troposphere during the latter period relative to the earlier period, consistent with the OMI observations. The most pronounced ozone increases were during the local biomass burning season (SON), with >30 ppb ozone increases below 850 hPa.

Figure S8 in Supporting Information S1 also compares the simulated ozone profiles driven by bottom-up and top-down emissions. At locations where observations indicated significant tropospheric ozone differences between the two periods, both simulations showed significant ozone changes. The use of different precursor emissions over Southeast Asia mainly affected the simulated ozone concentrations in the lower troposphere. Due

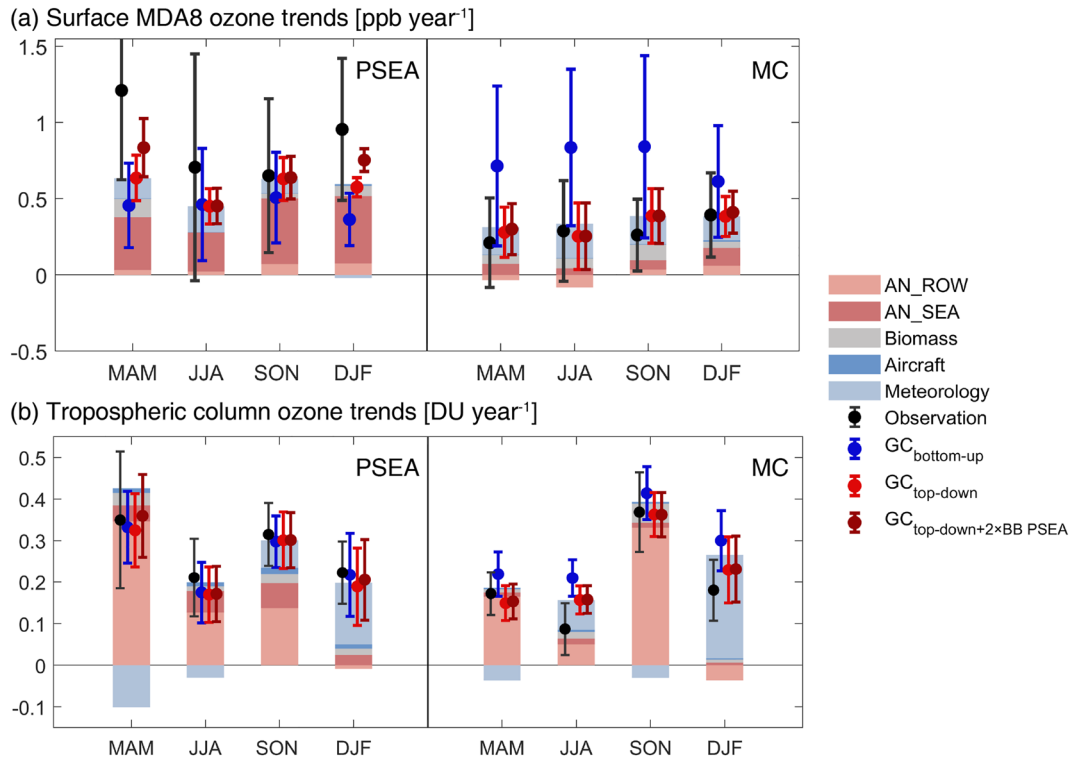


**Figure 4.** Driving factors contributing to (a) surface and (b) tropospheric ozone trends for the years between 2005 and 2016. Whiskers show surface or tropospheric ozone trends as observed (black) and as simulated with bottom-up emissions (blue), top-down emissions (light red), and top-down emissions plus a further increase of the biomass burning emission trends over the PSEA by a factor of two (dark red). Histogram shows the simulated contributions of individual drivers, including interannual variations of anthropogenic emission from Southeast Asia (AN_SEA) and the rest of the World (AN_ROW), biomass burning emissions (Biomass), aircraft emissions (Aircraft), and meteorology.

to the uncertainties in the lower-tropospheric ozone observations, we could not infer which simulation was more consistent with the observed ozone changes between the two periods.

## 5. Drivers of Surface and Tropospheric Ozone Changes Over Southeast Asia From 2005 to 2016

On the basis of our top-down simulation, Figure 4a, Figure S9 and Table S4 in Supporting Information S1 quantified the contributions of different drivers to the simulated ozone trends. Over the PSEA, 55%–72% of the simulated seasonal surface ozone trends were driven by anthropogenic emission growths in Southeast Asia. However, the top-down simulation still considerably underestimated the observed surface ozone trends over the PSEA, particularly during the local dry season. In contrast, the simulated modest surface ozone trends over the MC were profoundly affected by interannual variations of meteorology from 2005 to 2016 (41%–54% contribution). The rising anthropogenic and biomass burning emissions over Southeast Asia only contributed 10%–31% and 11%–27% of the seasonal surface ozone trends, respectively. The interannual variations of emissions from the rest of the world and global aviation had minor effects on the surface ozone trends over Southeast Asia.

Figure 4b, Figure S10 and Table S5 in Supporting Information S1 show the attributions of the TCO trends over the PSEA and MC. The rapid TCO increases over Southeast Asia were mostly driven by the anthropogenic emission growths from the rest of the World, which explained 71% of the simulated PSEA TCO trends in MAM and 79% of the simulated MC TCO trends in SON. TCO trends in DJF over both the PSEA and the MC were driven by interannual variations in meteorology, most likely that of ENSO. Strong El Niño events led to large-scale subsidence and high temperature over Southeast Asia, conducive to downward ozone transport from the stratosphere and tropospheric ozone formation (Oman et al., 2011; Sekiya & Sudo, 2012; Ziemke et al., 2010). Anthropogenic and biomass burning emissions from the Southeast Asia region contributed <11% of the simulated TCO trends

over the PSEA and the MC, which explained why the simulated TCO trends did not change much between bottom-up and top-down simulations.

## 6. Conclusion and Discussion

Our integrated analyses showed that surface and tropospheric ozone over Southeast Asia had risen from 2005 to 2016, with most substantial increases during the local biomass burning seasons (MAM in the PSEA and SON in the MC), and that current bottom-up inventories likely underestimated emission growths in the PSEA while overestimated emission growths in the MC. We also showed that the observed surface and tropospheric ozone trends were driven by a combination of emission growths within and outside Southeast Asia and interannual variations of meteorology. However, the pronounced surface ozone increases over the PSEA during the local dry season could not be fully accounted for even with our top-down emissions.

We hypothesized that the unexplained surface ozone trends over the PSEA might be due to underestimated growths of biomass burning emissions over the region. Biomass burning in the PSEA were primarily associated crop residue burning and likely increased with the growing crop production in that region (Oanh et al., 2018). Current fire inventories based on satellite-observations of burnt area or fire power systematically under-detect the small, smoldering fires associated with crop residue burning (Lasko et al., 2017; T. Liu et al., 2019; Randerson et al., 2012; T. Zhang et al., 2018). Although our top-down constraints scaled up the biomass burning emission trends over the PSEA, we were only able to enlarge emission growths at locations where burning emissions were already present in the inventory. The PSEA surface ozone measurements were mostly over Central and Western Thailand (Figure S1 in Supporting Information S1), but the fire emissions represented in the GFED4s inventory were mostly over Northern PSEA and Cambodia (Figure S11 in Supporting Information S1). If there were undetected burning over Central and Western Thailand, the magnitudes of biomass burning emissions may still be severely underestimated despite our scaling-up. We conducted another experiment based on top-down emissions but further increased the trends of biomass burning emissions over the PSEA by a factor of two. We found the simulated surface ozone trends would increase by 0.2 ppb year$^{-1}$ during the dry season over PSEA, which is more consistent with observations while still within the observed ranges of TCO trends (Figure 4).

We speculated what might have caused the CEDS to underestimate $NO_x$ emission growths over the PSEA. The CEDS $NO_x$ emissions from the PSEA energy sector grew only by 90% from 2005 to 2016, but another study (X. Chen & Mauzerall, 2021) showed that the power generation capacity had rapidly increased by approximately 150% from 2005 to 2016 over Southeast Asia. Conversely, the CEDS may have overestimated $NO_x$ emission growths over the MC. We traced this bias to the fast growths of the transport sector (Figure S12 in Supporting Information S1) in the REAS inventory version 2 between the years 2000 and 2008 (Kurokawa et al., 2013), which did not account for vehicular emission regulations successively put in place by Southeast Asian countries after 1996 (Clean Air Asia, 2011). The REAS inventory version 3 updated emission factors associated with new vehicle standards and showed a markedly slower $NO_x$ emission increase (31 Gg year$^{-1}$) in Southeast Asia after the year 2005 (Kurokawa & Ohara, 2020), similar to our top-down constrained $NO_x$ emissions. Other bottom-up inventories also showed diverse emission magnitudes and trends over Southeast Asia (Elguindi et al., 2020). For example, the global emission inventory EDGAR (Crippa et al., 2018) showed an MC $NO_x$ emission trend similar to that in REAS version 3 after 2007 but significantly underestimated the $NO_x$ trend before 2007, and its Southeast Asian $NO_x$ emissions were up to 50% lower than those in REAS version 3 (Elguindi et al., 2020). We demonstrated the need to better quantify the long-term changes of anthropogenic and biomass burning emissions in Southeast Asia, in order to better understand air quality changes and inform air quality management in this region.

## Data Availability Statement

Monthly surface ozone observations and our top-down $NO_x$ emissions over Southeast Asia are permanently archived at https://www.scidb.cn/en/s/3uIB3m. SHADOZ and IAGOS measurements can be downloaded from https://tropo.gsfc.nasa.gov/shadoz/Archive.html and https://iagos.aeris-data.fr/download/#/, respectively. OMI/SAO Level 2 Ozone Profile product are available at https://avdc.gsfc.nasa.gov/pub/data/satellite/Aura/OMI/V03/L2/OMPROFOZ/. OMI/MLS ozone products are available at https://acd-ext.gsfc.nasa.gov/Data_services/cloud_slice/new_data.html. OMI Level 2 tropospheric $NO_2$ products are downloadable at

https://doi.org/10.5067/Aura/OMI/DATA2017. The GEOS-Chem version 12.1.1 code used in this study can be downloaded from https://github.com/geoschem/GCClassic.

**Acknowledgments**
This work was supported by the Guangdong Basic and Applied Basic Research Fund (2020B1515130003), the Shenzhen Science and Technology Innovation Committee (KCXFZ202002011008038), and the National Natural Science Foundation of China (41922037). Computational resources were provided by the Center for Computational Science and Engineering at the Southern University of Science and Technology. We thank the Malaysian Department of Environment and the Thailand Pollution Control Department for the surface ozone measurements.

## References

Ahamad, F., Griffiths, P. T., Latif, M. T., Juneng, L., & Xiang, C. J. (2020). Ozone trends from two decades of ground level observation in Malaysia. *Atmosphere*, *11*(7), 755. https://doi.org/10.3390/atmos11070755

Amnuaylojaroen, T., Macatangay, R. C., & Khodmanee, S. (2019). Modeling the effect of VOCs from biomass burning emissions on ozone pollution in upper Southeast Asia. *Heliyon*, *5*(10), e02661. https://doi.org/10.1016/j.heliyon.2019.e02661

Ashfold, M. J., Latif, M. T., Samah, A. A., Mead, M. I., & Harris, N. R. P. (2017). Influence of Northeast Monsoon cold surges on air quality in Southeast Asia. *Atmospheric Environment*, *166*, 498–509. https://doi.org/10.1016/j.atmosenv.2017.07.047

Assareh, N., Prabamroong, T., Manomaiphiboon, K., Theramongkol, P., Leungsakul, S., Mitrjit, N., & Rachiwong, J. (2016). Analysis of observed surface ozone in the dry season over Eastern Thailand during 1997–2012. *Atmospheric Research*, *178–179*, 17–30. https://doi.org/10.1016/j.atmosres.2016.03.009

Austin, K. G., Schwantes, A., Gu, Y., & Kasibhatla, P. S. (2019). What causes deforestation in Indonesia? *Environmental Research Letters*, *14*(2), 024007. https://doi.org/10.1088/1748-9326/aaf6db

Bey, I., Jacob, D. J., Yantosca, R. M., Logan, J. A., Field, B. D., Fiore, A. M., et al. (2001). Global modeling of tropospheric chemistry with assimilated meteorology: Model description and evaluation. *Journal of Geophysical Research*, *106*(D19), 23073–23095. https://doi.org/10.1029/2001JD000807

Chen, X., & Mauzerall, D. L. (2021). The expanding coal power fleet in Southeast Asia: Implications for future $CO_2$ emissions and electricity generation. *Earth's Future*, *9*(12), e2021EF002257. https://doi.org/10.1029/2021EF002257

Chen, Y., Morton, D. C., Andela, N., van der Werf, G. R., Giglio, L., & Randerson, J. T. (2017). A pan-tropical cascade of fire driven by El Niño/Southern Oscillation. *Nature Climate Change*, *7*(12), 906–911. https://doi.org/10.1038/s41558-017-0014-8

Clean Air Asia. (2011). Road map to cleaner fuels and vehicles in Asia, factsheet No. 17. *Clean Air Initiative for Asian Cities Center-Asia*. Retrieved from https://www.cleanairinitiative.org/portal/knowledgebase/publications/

Crippa, M., Guizzardi, D., Muntean, M., Schaaf, E., Dentener, F., van Aardenne, J. A., et al. (2018). Gridded emissions of air pollutants for the period 1970–2012 within EDGAR v4.3.2. *Earth System Science Data*, *10*(4), 1987–2013. https://doi.org/10.5194/essd-10-1987-2018

Elguindi, N., Granier, C., Stavrakou, T., Darras, S., Bauwens, M., Cao, H., et al. (2020). Intercomparison of magnitudes and trends in anthropogenic surface emissions from bottom-up inventories, top-down estimates, and emission scenarios. *Earth's Future*, *8*(8), e2020EF001520. https://doi.org/10.1029/2020EF001520

Gaudel, A., Cooper, O. R., Ancellet, G., Barret, B., Boynard, A., Burrows, J. P., et al. (2018). Tropospheric Ozone Assessment Report: Present-day distribution and trends of tropospheric ozone relevant to climate and global atmospheric chemistry model evaluation. *Elementa: Science of the Anthropocene*, *6*, 39. https://doi.org/10.1525/elementa.291

Gaudel, A., Cooper, O. R., Chang, K.-L., Bourgeois, I., Ziemke, J. R., Strode, S. A., et al. (2020). Aircraft observations since the 1990s reveal increases of tropospheric ozone at multiple locations across the Northern Hemisphere. *Science Advances*, *6*(34), eaba8272. https://doi.org/10.1126/sciadv.aba8272

Gelaro, R., McCarty, W., Suárez, M. J., Todling, R., Molod, A., Takacs, L., et al. (2017). The Modern-Era retrospective analysis for Research and Applications, version 2 (MERRA-2). *Journal of Climate*, *30*(14), 5419–5454. https://doi.org/10.1175/JCLI-D-16-0758.1

Georgoulias, A. K., van der A, R. J., Stammes, P., Boersma, K. F., & Eskes, H. J. (2019). Trends and trend reversal detection in 2 decades of tropospheric $NO_2$ satellite observations. *Atmospheric Chemistry and Physics*, *19*(9), 6269–6294. https://doi.org/10.5194/acp-19-6269-2019

Goldberg, D. L., Anenberg, S. C., Lu, Z., Streets, D. G., Lamsal, L. N., McDuffie, E., & Smith, S. J. (2021). Urban $NO_x$ emissions around the world declined faster than anticipated between 2005 and 2019. *Environmental Research Letters*, *16*(11), 115004. https://doi.org/10.1088/1748-9326/ac2c34

Guenther, A. B., Jiang, X., Heald, C. L., Sakulyanontvittaya, T., Duhl, T., Emmons, L. K., & Wang, X. (2012). The model of emissions of gases and aerosols from nature version 2.1 (MEGAN2.1): An extended and updated framework for modeling biogenic emissions. *Geoscientific Model Development*, *5*(6), 1471–1492. https://doi.org/10.5194/gmd-5-1471-2012

Holmes, C. D., Prather, M. J., & Vinken, G. C. M. (2014). The climate impact of ship $NO_x$ emissions: An improved estimate accounting for plume chemistry. *Atmospheric Chemistry and Physics*, *14*(13), 6801–6812. https://doi.org/10.5194/acp-14-6801-2014

Huang, G., Liu, X., Chance, K., Yang, K., Bhartia, P. K., Cai, Z., et al. (2017). Validation of 10-year SAO OMI Ozone Profile (PROFOZ) product using ozonesonde observations. *Atmospheric Measurement Techniques*, *10*(7), 2455–2475. https://doi.org/10.5194/amt-10-2455-2017

Hudman, R. C., Moore, N. E., Mebust, A. K., Martin, R. V., Russell, A. R., Valin, L. C., & Cohen, R. C. (2012). Steps towards a mechanistic model of global soil nitric oxide emissions: Implementation and space based-constraints. *Atmospheric Chemistry and Physics*, *12*(16), 7779–7795. https://doi.org/10.5194/acp-12-7779-2012

Intergovernmental Panel on Climate Change (IPCC). (2021). Climate change 2021: The physical science basis. In V. Masson-Delmotte, P. Zhai, A. Pirani, S. L. Connors, C. Péan, S. Berger, et al. (Eds.), *Contribution of working group I to the sixth assessment report of the intergovernmental panel on climate change*. Cambridge University Press. Retrieved from https://www.ipcc.ch/report/ar6/wg1/downloads/report/IPCC_AR6_WGI_Full_Report_smaller.pdf.2338

International Energy Agency (IEA). (2019). Southeast Asia energy outlook 2019. *IEA*. Retrieved from https://www.iea.org/reports/southeast-asia-energy-outlook-2019

Jian, Y., & Fu, T.-M. (2014). Injection heights of springtime biomass-burning plumes over peninsular Southeast Asia and their impacts on long-range pollutant transport. *Atmospheric Chemistry and Physics*, *14*(8), 3977–3989. https://doi.org/10.5194/acp-14-3977-2014

Khodmanee, S., & Amnuaylojaroen, T. (2021). Impact of biomass burning on ozone, carbon monoxide, and nitrogen dioxide in Northern Thailand. *Frontiers in Environmental Science*, *9*, 641877. https://doi.org/10.3389/fenvs.2021.641877

Krotkov, N. A., Lamsal, L. N., Celarier, E. A., Swartz, W. H., Marchenko, S. V., Bucsela, E. J., et al. (2017). The version 3 OMI $NO_2$ standard product. *Atmospheric Measurement Techniques*, *10*(9), 3133–3149. https://doi.org/10.5194/amt-10-3133-2017

Kurokawa, J., & Ohara, T. (2020). Long-term historical trends in air pollutant emissions in Asia: Regional emission inventory in Asia (REAS) version 3. *Atmospheric Chemistry and Physics*, *20*(21), 12761–12793. https://doi.org/10.5194/acp-20-12761-2020

Kurokawa, J., Ohara, T., Morikawa, T., Hanayama, S., Janssens-Maenhout, G., Fukui, T., et al. (2013). Emissions of air pollutants and greenhouse gases over Asian regions during 2000–2008: Regional emission inventory in Asia (REAS) version 2. *Atmospheric Chemistry and Physics*, *13*(21), 11019–11058. https://doi.org/10.5194/acp-13-11019-2013

Lasko, K., Vadrevu, K. P., Tran, V. T., Ellicott, E., Nguyen, T. T. N., Bui, H. Q., & Justice, C. (2017). Satellites may underestimate rice residue and associated burning emissions in Vietnam. *Environmental Research Letters*, *12*(8), 085006. https://doi.org/10.1088/1748-9326/aa751d

Latif, M. T., Dominick, D., Ahamad, F., Ahamad, N. S., Khan, M. F., Juneng, L., et al. (2016). Seasonal and long term variations of surface ozone concentrations in Malaysian Borneo. *Science of the Total Environment*, *573*, 494–504. https://doi.org/10.1016/j.scitotenv.2016.08.121

Liu, T., Marlier, M. E., Karambelas, A., Jain, M., Singh, S., Singh, M. K., et al. (2019). Missing emissions from post-monsoon agricultural fires in northwestern India: Regional limitations of MODIS burned area and active fire products. *Environmental Research Communications*, *1*(1), 011007. https://doi.org/10.1088/2515-7620/ab056c

Liu, X., Bhartia, P. K., Chance, K., Spurr, R. J. D., & Kurosu, T. P. (2010). Ozone profile retrievals from the ozone monitoring instrument. *Atmospheric Chemistry and Physics*, *10*(5), 2521–2537. https://doi.org/10.5194/acp-10-2521-2010

Lu, X., Zhang, L., Wang, X., Gao, M., Li, K., Zhang, Y., et al. (2020). Rapid increases in warm-season surface ozone and resulting health impact in China since 2013. *Environmental Science and Technology Letters*, *7*(4), 240–247. https://doi.org/10.1021/acs.estlett.0c00171

Mao, J., Fan, S., Jacob, D. J., & Travis, K. R. (2013). Radical loss in the atmosphere from Cu-Fe redox coupling in aerosols. *Atmospheric Chemistry and Physics*, *13*(2), 509–519. https://doi.org/10.5194/acp-13-509-2013

Marvin, M. R., Palmer, P. I., Latter, B. G., Siddans, R., Kerridge, B. J., Latif, M. T., & Khan, M. F. (2021). Photochemical environment over Southeast Asia primed for hazardous ozone levels with influx of nitrogen oxides from seasonal biomass burning. *Atmospheric Chemistry and Physics*, *21*(3), 1917–1935. https://doi.org/10.5194/acp-21-1917-2021

McDuffie, E. E., Smith, S. J., O'Rourke, P., Tibrewal, K., Venkataraman, C., Marais, E. A., et al. (2020). A global anthropogenic emission inventory of atmospheric pollutants from sector- and fuel-specific sources (1970–2017): An application of the community emissions data system (CEDS). *Earth System Science Data*, *12*(4), 3413–3442. https://doi.org/10.5194/essd-12-3413-2020

McLinden, C. A., Olsen, S. C., Hannegan, B., Wild, O., Prather, M. J., & Sundet, J. (2000). Stratospheric ozone in 3-D models: A simple chemistry and the cross-tropopause flux. *Journal of Geophysical Research*, *105*(D11), 14653–14665. https://doi.org/10.1029/2000JD900124

Monks, P. S., Archibald, A. T., Colette, A., Cooper, O., Coyle, M., Derwent, R., et al. (2015). Tropospheric ozone and its precursors from the urban to the global scale from air quality to short-lived climate forcer. *Atmospheric Chemistry and Physics*, *15*(15), 8889–8973. https://doi.org/10.5194/acp-15-8889-2015

Murray, L. T., Jacob, D. J., Logan, J. A., Hudman, R. C., & Koshak, W. J. (2012). Optimized regional and interannual variability of lightning in a global chemical transport model constrained by LIS/OTD satellite data. *Journal of Geophysical Research*, *117*(D20), D20307. https://doi.org/10.1029/2012JD017934

Nédélec, P., Blot, R., Boulanger, D., Athier, G., Cousin, J.-M., Gautron, B., et al. (2015). Instrumentation on commercial aircraft for monitoring the atmospheric composition on a global scale: The IAGOS system, technical overview of ozone and carbon monoxide measurements. *Tellus B: Chemical and Physical Meteorology*, *67*(1), 27791. https://doi.org/10.3402/tellusb.v67.27791

Oanh, N. T. K., Permadi, D. A., Hopke, P. K., Smith, K. R., Dong, N. P., & Dang, A. N. (2018). Annual emissions of air toxics emitted from crop residue open burning in Southeast Asia over the period of 2010–2015. *Atmospheric Environment*, *187*, 163–173. https://doi.org/10.1016/j.atmosenv.2018.05.061

Olsen, M. A., Wargan, K., & Pawson, S. (2016). Tropospheric column ozone response to ENSO in GEOS-5 assimilation of OMI and MLS ozone data. *Atmospheric Chemistry and Physics*, *16*(11), 7091–7103. https://doi.org/10.5194/acp-16-7091-2016

Oman, L. D., Douglass, A. R., Ziemke, J. R., Rodriguez, J. M., Waugh, D. W., & Nielsen, J. E. (2013). The ozone response to ENSO in Aura satellite measurements and a chemistry-climate simulation. *Journal of Geophysical Research: Atmospheres*, *118*(2), 965–976. https://doi.org/10.1029/2012JD018546

Oman, L. D., Ziemke, J. R., Douglass, A. R., Waugh, D. W., Lang, C., Rodriguez, J. M., & Nielsen, J. E. (2011). The response of tropical tropospheric ozone to ENSO. *Geophysical Research Letters*, *38*(13), L13706. https://doi.org/10.1029/2011GL047865

O'Rourke, P. R., Smith, S. J., Mott, A., Ahsan, H., McDuffie, E. E., Crippa, M., et al. (2021). CEDS v_2021-04-21 emission data 1975-2019 (version April-21-2021). *Zenodo*. https://doi.org/10.5281/zenodo.3592072

Petzold, A., Thouret, V., Gerbig, C., Zahn, A., Brenninkmeijer, C. A. M., Gallagher, M., et al. (2015). Global-scale atmosphere monitoring by in-service aircraft–current achievements and future prospects of the European Research Infrastructure IAGOS. *Tellus B: Chemical and Physical Meteorology*, *67*(1), 28452. https://doi.org/10.3402/tellusb.v67.28452

Randerson, J. T., Chen, Y., van der Werf, G. R., Rogers, B. M., & Morton, D. C. (2012). Global burned area and biomass burning emissions from small fires. *Journal of Geophysical Research*, *117*(G4), G04012. https://doi.org/10.1029/2012JG002128

Reddington, C. L., Conibear, L., Robinson, S., Knote, C., Arnold, S. R., & Spracklen, D. V. (2021). Air pollution from forest and vegetation fires in Southeast Asia disproportionately impacts the poor. *GeoHealth*, *5*(9), e2021GH000418. https://doi.org/10.1029/2021GH000418

Sekiya, T., & Sudo, K. (2012). Role of meteorological variability in global tropospheric ozone during 1970–2008. *Journal of Geophysical Research*, *117*(D18), D18303. https://doi.org/10.1029/2012JD018054

Sherwen, T., Schmidt, J. A., Evans, M. J., Carpenter, L. J., Großmann, K., Eastham, S. D., et al. (2016). Global impacts of tropospheric halogens (Cl, Br, I) on oxidants and composition in GEOS-Chem. *Atmospheric Chemistry and Physics*, *16*(18), 12239–12271. https://doi.org/10.5194/acp-16-12239-2016

Thompson, A. M., Witte, J. C., Sterling, C., Jordan, A., Johnson, B. J., Oltmans, S. J., et al. (2017). First reprocessing of southern Hemisphere additional ozonesondes (SHADOZ) ozone profiles (1998–2016): 2. Comparisons with satellites and ground-based instruments. *Journal of Geophysical Research: Atmospheres*, *122*(23), 13000–13025. https://doi.org/10.1002/2017JD027406

van der Werf, G. R., Dempewolf, J., Trigg, S. N., Randerson, J. T., Kasibhatla, P. S., Giglio, L., et al. (2008). Climate regulation of fire emissions and deforestation in equatorial Asia. *Proceedings of the National Academy of Sciences of the United States of America*, *105*(51), 20350–20355. https://doi.org/10.1073/pnas.0803375105

van der Werf, G. R., Randerson, J. T., Giglio, L., van Leeuwen, T. T., Chen, Y., Rogers, B. M., et al. (2017). Global fire emissions estimates during 1997–2016. *Earth System Science Data*, *9*(2), 697–720. https://doi.org/10.5194/essd-9-697-2017

Wang, T., Dai, J., Lam, K. S., Poon, C. N., & Brasseur, G. P. (2019). Twenty-five years of lower tropospheric ozone observations in tropical East Asia: The influence of emissions and weather patterns. *Geophysical Research Letters*, *46*(20), 11463–11470. https://doi.org/10.1029/2019GL084459

Witte, J. C., Thompson, A. M., Smit, H. G. J., Fujiwara, M., Posny, F., Coetzee, G. J. R., et al. (2017). First reprocessing of southern Hemisphere additional ozonesondes (SHADOZ) profile records (1998-2015): 1. Methodology and evaluation. *Journal of Geophysical Research: Atmospheres*, *122*(12), 6611–6636. https://doi.org/10.1002/2016JD026403

Witte, J. C., Thompson, A. M., Smit, H. G. J., Vömel, H., Posny, F., & Stübi, R. (2018). First reprocessing of southern Hemisphere additional ozonesondes profile records: 3. Uncertainty in ozone profile and total column. *Journal of Geophysical Research: Atmospheres*, *123*(6), 3243–3268. https://doi.org/10.1002/2017JD027791

Zhang, L., Jacob, D. J., Liu, X., Logan, J. A., Chance, K., Eldering, A., & Bojkov, B. R. (2010). Intercomparison methods for satellite measurements of atmospheric composition: Application to tropospheric ozone from TES and OMI. *Atmospheric Chemistry and Physics*, *10*(10), 4725–4739. https://doi.org/10.5194/acp-10-4725-2010

Zhang, T., Wooster, M. J., Jong De, M. C., & Xu, W. (2018). How well does the 'Small Fire Boost' methodology used within the GFED4.1s fire emissions database represent the timing, location and magnitude of agricultural burning? *Remote Sensing*, *10*(6), 823. https://doi.org/10.3390/rs10060823

Zhang, Y., Cooper, O. R., Gaudel, A., Thompson, A. M., Nédélec, P., Ogino, S.-Y., & West, J. J. (2016). Tropospheric ozone change from 1980 to 2010 dominated by equatorward redistribution of emissions. *Nature Geoscience*, *9*(12), 875–879. https://doi.org/10.1038/ngeo2827

Zhang, Y., West, J. J., Emmons, L. K., Flemming, J., Jonson, J. E., Lund, M. T., et al. (2021). Contributions of world regions to the global tropospheric ozone burden change from 1980 to 2010. *Geophysical Research Letters*, *48*(1), e2020GL089184. https://doi.org/10.1029/2020GL089184

Ziemke, J. R., Chandra, S., Oman, L. D., & Bhartia, P. K. (2010). A new ENSO index derived from satellite measurements of column ozone. *Atmospheric Chemistry and Physics*, *10*(8), 3711–3721. https://doi.org/10.5194/acp-10-3711-2010

Ziemke, J. R., Oman, L. D., Strode, S. A., Douglass, A. R., Olsen, M. A., McPeters, R. D., et al. (2019). Trends in global tropospheric ozone inferred from a composite record of TOMS/OMI/MLS/OMPS satellite measurements and the MERRA-2 GMI simulation. *Atmospheric Chemistry and Physics*, *19*(5), 3257–3269. https://doi.org/10.5194/acp-19-3257-2019

## References From the Supporting Information

Fujiwara, M., Kita, K., Kawakami, S., Ogawa, T., Komala, N., Saraspriya, S., & Suripto, A. (1999). Tropospheric ozone enhancements during the Indonesian Forest Fire Events in 1994 and in 1997 as revealed by ground-based observations. *Geophysical Research Letters*, *26*(16), 2417–2420. https://doi.org/10.1029/1999GL900117

He, J., Gong, S., Yu, Y., Yu, L., Wu, L., Mao, H., et al. (2017). Air pollution characteristics and their relation to meteorological conditions during 2014–2015 in major Chinese cities. *Environmental Pollution*, *223*, 484–496. https://doi.org/10.1016/j.envpol.2017.01.050

Lamsal, L. N., Martin, R. V., Padmanabhan, A., van Donkelaar, A., Zhang, Q., Sioris, C. E., et al. (2011). Application of satellite observations for timely updates to global anthropogenic NOx emission inventories. *Geophysical Research Letters*, *38*(5), L05810. https://doi.org/10.1029/2010GL046476

Levelt, P. F., van den Oord, G. H. J., Dobber, M. R., Malkki, A., Visser, H., Vries, J., et al. (2006). The ozone monitoring instrument. *IEEE Transactions on Geoscience and Remote Sensing*, *44*(5), 1093–1101. https://doi.org/10.1109/TGRS.2006.872333

Li, M., Liu, H., Geng, G., Hong, C., Liu, F., Song, Y., et al. (2017). Anthropogenic emission inventories in China: A review. *National Science Review*, *4*(6), 834–866. https://doi.org/10.1093/nsr/nwx150

McPeters, R. D., Labow, G. J., & Logan, J. A. (2007). Ozone climatological profiles for satellite retrieval algorithms. *Journal of Geophysical Research*, *112*(D5), D05308. https://doi.org/10.1029/2005JD006823

Schoeberl, M. R., Douglass, A. R., Hilsenrath, E., Bhartia, P. K., Beer, R., Waters, J. W., et al. (2006). Overview of the EOS aura mission. *IEEE Transactions on Geoscience and Remote Sensing*, *44*(5), 1066–1074. https://doi.org/10.1109/TGRS.2005.861950

Schultz, M. G., Schröder, S., Lyapina, O., Cooper, O., Galbally, I., Petropavlovskikh, I., et al. (2017). Tropospheric ozone assessment report: Database and metrics data of global surface ozone observations. *Elementa: Science of the Anthropocene*, *5*, 58. https://doi.org/10.1525/elementa.244

Sterling, C. W., Johnson, B. J., Oltmans, S. J., Smit, H. G. J., Jordan, A. F., Cullis, P. D., et al. (2018). Homogenizing and estimating the uncertainty in NOAA's long-term vertical ozone profile records measured with the electrochemical concentration cell ozonesonde. *Atmospheric Measurement Techniques*, *11*(6), 3661–3687. https://doi.org/10.5194/amt-11-3661-2018

van der Werf, G. R., Randerson, J. T., Giglio, L., Collatz, G. J., Mu, M., Kasibhatla, P. S., et al. (2010). Global fire emissions and the contribution of deforestation, savanna, forest, agricultural, and peat fires (1997–2009). *Atmospheric Chemistry and Physics*, *10*(23), 11707–11735. https://doi.org/10.5194/acp-10-11707-2010

Zheng, B., Tong, D., Li, M., Liu, F., Hong, C., Geng, G., et al. (2018). Trends in China's anthropogenic emissions since 2010 as the consequence of clean air actions. *Atmospheric Chemistry and Physics*, *18*(19), 14095–14111. https://doi.org/10.5194/acp-18-14095-2018